Subsurface ocean argon disequilibrium reveals the equatorial Pacific shadow zone

Eric Gehrie,[1] David Archer,[1] Steven Emerson,[2] Charles Stump,[2] and Cara Henning[3]

[1] Surface water in the ocean invades the subsurface vertically, against the density gradient, and along constant-density surfaces from surface outcrops in high latitudes. We present dissolved argon data that distinguishes a diapycnally ventilated upper thermocline in the equatorial Pacific versus an isopycnally ventilated subtropical location near Hawaii. The lower thermocline is shown to be isopycnally ventilated at both locations, in contrast with theoretical and model predictions. **Citation:** Gehrie, E., D. Archer, S. Emerson, C. Stump, and C. Henning (2006), Subsurface ocean argon disequilibrium reveals the equatorial Pacific shadow zone, *Geophys. Res. Lett.*, *33*, L18608, doi:10.1029/2006GL026935.

1. Introduction

[2] The chemistry of seawater is altered at the sea surface by exchange of naturally occurring atmospheric gases such as O_2, CO_2, and Ar. The atmospheric imprint on seawater is carried into the ocean interior by fluid flow from the Ekman layer and by mixing, processes known collectively as "ventilation". Pathways and mechanisms of ocean ventilation determine the circulation of the thermocline and affect the ocean response to climate change, uptake of anthropogenic CO_2, and the distribution of oxygen and nutrients in subsurface waters.

[3] Some parts of the subsurface ocean (e.g. the subtropics) are ventilated by fluid flow. *Luyten et al.* [1983] postulated that after a fluid parcel is isolated from the atmosphere, its trajectory is governed by conservation of potential vorticity. In oceanic "shadow zones" like the equatorial Pacific, vorticity-conserving fluid flow trajectories intersect the boundaries of the ocean or close in upon themselves, rather than outcropping at the sea surface. Ventilation of shadow zones takes place via eddy or turbulent diffusion, either in the vertical (diapycnal) direction or along isopycnal surfaces.

[4] Within shadow zones, it has been difficult to clearly differentiate the processes of diapycnal versus isopycnal ventilation. Freon concentration provides a marker of a recent atmospheric imprint on subsurface ocean waters [see *Fine et al.*, 2001], but is ambiguous with regard to pathway. *Walin* [1982], *Speer* [1997], and *Nurser et al.* [1999] reason that the production of thermocline fluid by Ekman pumping into the thermocline from the subtropical sea surface must be balanced by loss of thermocline fluid to diapycnal mixing. *Nurser et al.* [1999] verified in a high-resolution isopycnic model (Micom) of the Atlantic Ocean that diapycnal diffusion balances Ekman pumping, and found that most of the required mixing is taking place in the equatorial thermocline where thermal gradients are steepest.

[5] The distribution of stable noble gases such as argon may provide a measure of subsurface diapycnal mixing. The solubility of argon is nonlinear with temperature (Figure 1), so that mixing of equilibrated waters of different temperatures produces supersaturation [*Hamme and Emerson*, 2004]. Ocean circulation models predict measurable argon supersaturation in shadow zones where ventilation is predominantly diapycnal [see *Henning et al.*, 2006; *Ito and Deutsch*, 2006]. Supersaturation accumulates over the subsurface lifetime of a water parcel, and is thermodynamically stabilized by increased pressure at depth. In our experiments, the POP and Micom ocean circulation models clearly see the equatorial thermocline as a diapycnally ventilated shadow zone (Figure 2). Previously available argon data from the 1960s and 70s are too inaccurate to test this prediction [see *Bieri et al.*, 1966; *Craig et al.*, 1967; *Bieri*, 1971; *Bieri and Koide*, 1972]. We present new data from the equatorial Pacific Ocean.

2. Methods

2.1. Measurement

[6] Samples were collected aboard National Oceanic and Atmospheric Administration (NOAA) ship *Ka'imimoana* in the same fashion as *Emerson et al.* [1999]. Four eastern equatorial Pacific sampling sites were selected based on the model results summarized in Figure 2: 8N at 110W, the equator at 110W, 8S at 95W, and 1S at 95W. Each station consisted of one deep cast and one shallow cast performed consecutively to minimize sampling time and the potential effects of heating on deck. The first three profiles sampled from both the deep abyss and the thermocline. The last site reached a maximum depth of 1000 meters. Argon samples were drawn in duplicate.

[7] Argon saturation values were determined by isotope dilution and solubility equations derived by *Hamme and Emerson* [2004]. The mean standard deviation of replicate measurements from the same Niskin bottle (n = 35) was ±0.2%.

2.2. Models

[8] The POP depth-coordinate General Circulation Model (GCM) was run at 3° longitudinal resolution and 1.4° latitudinal resolution with tighter grid spacing at the equator. The deep ocean was equilibrated over 2000 years with a base

---

[1]Department of the Geophysical Sciences, University of Chicago, Chicago, Illinois, USA.
[2]School of Oceanography, University of Washington, Seattle, Washington, USA.
[3]Department of Earth and Planetary Sciences, University of California, Berkeley, California, USA.
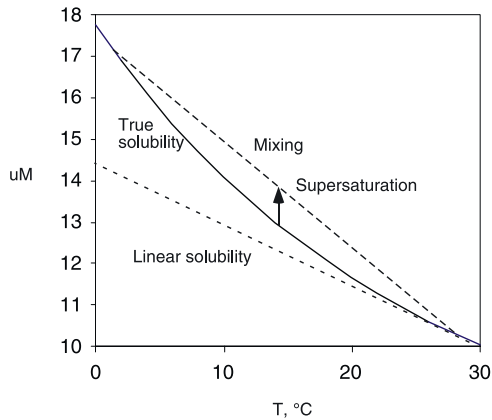
Figure 1. Solubility of argon as a function of temperature (solid line), mixing of saturated water parcels of different temperatures generates supersaturation (long-dashed line), and the linear solubility relation used in some model runs (short-dashed line).

case background diffusivity of 3×10^{-5} m^2/s. Beginning from this initial condition, the model was integrated for a further 100 years using three values of the background mixing scheme: high (1×10^{-4} m^2/s), base, and low (1×10^{-5} m^2/s). The model used the *Gent and McWilliams* [1990] isopycnal mixing scheme. In contrast to *Henning et al.* [2006], these runs used a realistic value for gas exchange, allowing the sea surface to depart from equilibrium. Most of the runs did not include the effects of bubble injection, except for one run that used base diffusivity and offset the gas exchange algorithm to simulate 1% steady-state supersaturation due to bubbles at the surface.

[9] We also show results from the Micom isopycnic-coordinate model [see *Bleck*, 1998]. This model is formulated with a vertical grid following isopycnal surfaces, eliminating the need for any cross-grid flow except where mixing is explicitly required, thereby eliminating numerical mixing across isopycnal surfaces. Temperature is not conserved with fluid flow, so we created a passive tracer temperature that is advected conservatively alongside argon. After 100 years of simulation, the largest deviation in the Pacific between active and passive temperature fields was about 4°C, in thermocline waters of the western equatorial warm pool. Both models show supersaturation in the equatorial thermocline, ruling out numerical vertical diffusion as the source of the mixing in the z-coordinate POP model. Surprisingly, the thermocline in Micom is more supersaturated than it is in POP or in the real ocean. Henceforth we restrict our attention to results of the POP model.

3. Results

[10] The data are plotted in Figures 3 and 4, along with data from the Hawaii Ocean Time-series (HOT) site, shown in grey for comparison. The temperature structure differs between Hawaii and the equator, reflecting the upward bowing of isopycnal surfaces at the equator drawn by upwelling. The temperature and salinity signatures of the subsurface waters differ (Figure 3b), with a more pronounced salinity minimum in Hawaii. The same argon

disequilibrium data are shown in all six plots of Figure 4 for comparison with model results.

[11] Both the equatorial and HOT datasets show undersaturation (-1 to -2.5%) in the abyss, which *Hamme and Emerson* [2002] attributed to convection outpacing gas exchange just prior to deep water formation in high latitude regions. At the surface both datasets feature moderate super saturation (less than 2% in the equatorial Pacific, less than 1% at HOT). Surface supersaturation is attributable to mechanisms of bubble injection or solar surface heating.

[12] The important difference between the sites is found in the thermocline. At the equatorial sites a distinct 2–3% argon supersaturation is observed between 15 and 25°C whereas HOT features only a few points between 15 and 25 °C that are more than 1% supersaturated. This difference is consistent with the predictions of POP and Micom ocean circulation models (Figures 2a and 2c).

[13] Before examining the GCM results in detail, we can compare the measured argon disequilibrium values against a simple case of pure mixing, as shown in Figure 1. If we postulate mixing between end members of 28°, 1% supersaturated at the surface and 10° C, saturated below, we predict a saturation maximum of about 3% at a temperature of 19°C. This scenario is represented by the blue curve in Figure 4a. Importantly, the pure mixing model coincides with the data from the equatorial Pacific, but not from Hawaii. This finding demonstrates the different ventilation mechanisms at work in the equatorial Pacific versus Hawaii.

[14] Concurrence between the equatorial Pacific data and the simple pure mixing model could simply be a coincidence because subsurface heating by penetrating solar radiation may also produce an argon supersaturation maximum at the base of the mixed layer. Because subsurface mixing generates argon disequilibrium as a consequence of the nonlinear relationship between argon solubility and temperature (Figure 1), the effect of subsurface heating in the model can be isolated from the effect of mixing by formulating a linear solubility for argon with temperature (Figure 2b). We therefore linearized the solubility equation around a temperature of 25°C, so that sea surface disequilibrium in equatorial waters due to heating remained close to the standard GCM run value of about 1%. In the linearized saturation case (red curve, Figures 4a and 4c). ΔAr% is near zero below 100 meters depth, and cooler than 20°C. The maximum ΔAr% is about 2%, at 50 meters depth. The observed disequilbrium values are higher than this, ranging from 2 to 4%, and at deeper depths, ranging from 50 to 100 meters. The data therefore show more supersaturation than predicted by the POP model for subsurface heating alone. Neither the data nor the model predicts much subsurface heating signature near the HOT site.

[15] The heat flux formulation in our POP model runs was forced as Jerlov type III water, with radiation penetration of 50 meters [*Jerlov*, 1976]. This formulation exceeds by a significant margin the heat penetration indicated by satellite ocean color data [see *Murtugudde et al.*, 2002]. The POP model results therefore nominally include the effects of subsurface heating by penetrating solar radiation, in addition to the effects of subsurface mixing (Figure 2a).

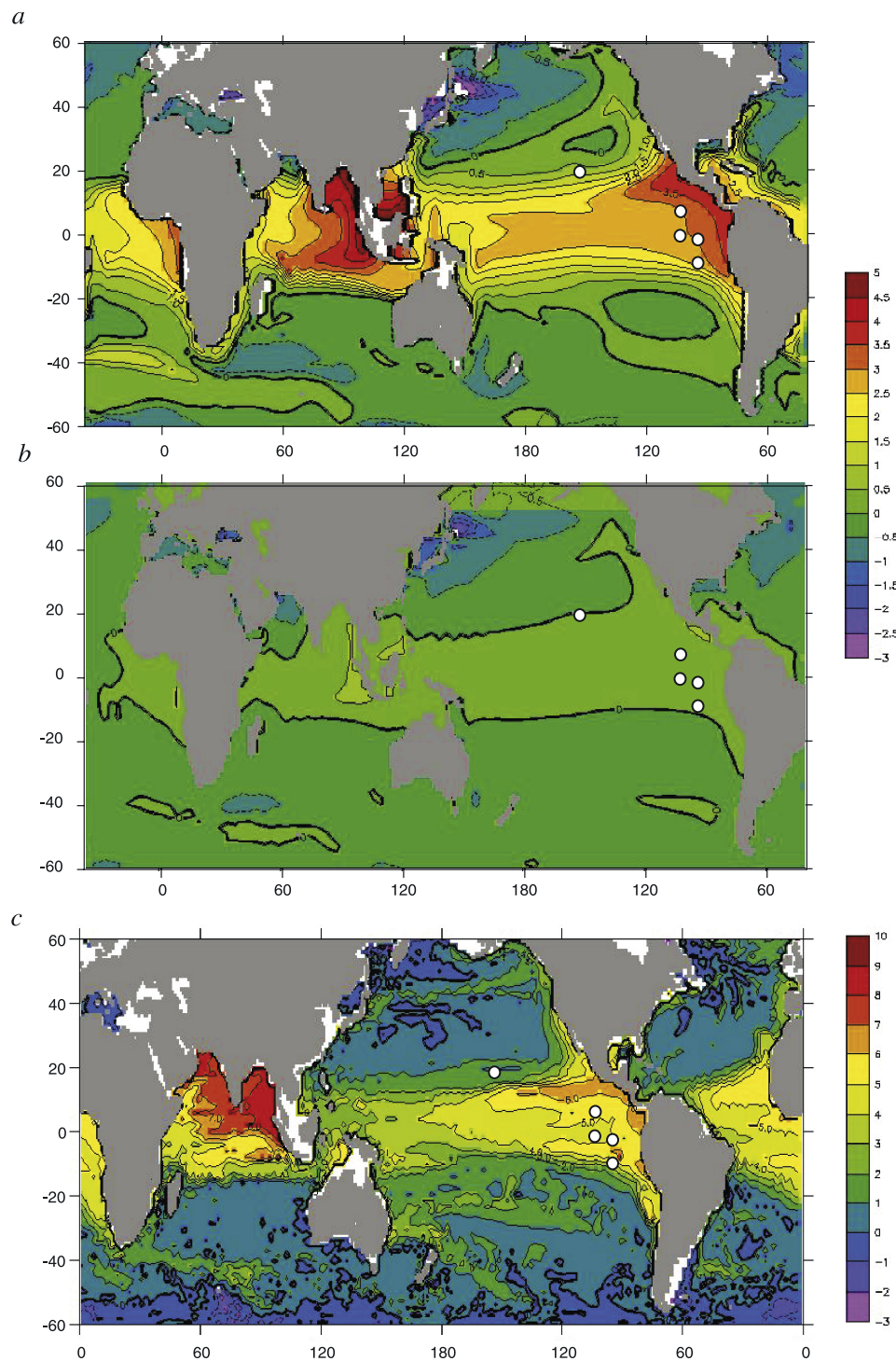[16] When we compare the data to results from the POP model that include the non-linear solubility of argon, we see

Figure 2. Subsurface argon disequilibrium in ocean circulation models: (a) POP model, 183 meters depth, (b) as in (a), but using linear saturation, which eliminates the mixing component of subsurface argon disequilibrium, and (c) Micom model, interpolated to 150 meters depth.

an increase in argon supersaturation throughout the water column, attributable to the effects of diapycnal mixing (Figure 4b). The fit to equatorial argon data in the shallow thermocline is improved relative to the linearized model, but the model predicts supersaturation in the deep thermocline that is not observed in the data. The temperature range of 10° to 5°C corresponds roughly to the "lower thermocline" waters which *Samelson and Vallis* [1997] predicted must be ventilated by diffusion, because this water outcrops in the subpolar gyre where the Ekman pumping is upward. The theory apparently works well to explain the model results, but not the real ocean. It could be that the deep thermocline

is actually ventilated by advection of Antarctic intermediate water, a process that is very difficult to capture in models. Alternatively, isopycnal eddy advection (diffusion) may be underestimated by the model.

[17] We can more easily evaluate mixing in the shallow thermocline in the model if we specify that argon shall be in equilibrium with saturation values in waters colder than 10°C (Figure 4c). When this is done, we see that the model profiles in the equatorial region reproduce the supersaturation extent and depth/temperature range of the data. The GCM profiles appear to be the sum of the profiles for theoretical mixing and subsurface heating.

[18] The density of seawater is determined by a combination of temperature and salinity, so eddy diffusion along an isopycnal surface could bring together waters of different temperature, generating some argon supersaturation. However, assuming a maximum salinity contrast of 2.0 PSU, we calculate that along-isopycnal diffusion could be responsible for no more than 0.5% of the observed argon supersaturation maximum.

[19] Another potential complicating effect is bubbles. Bubbles act to supersaturate the surface waters with respect to atmospheric gases by equilibrating at pressures higher than atmospheric pressure. The extent of bubble injection can be estimated using multiple gases with different solubility, such as argon and neon [see *Hamme and Emerson*, 2002]. Such data does not exist for the equatorial Pacific, but bubbles may account for 1% supersaturation at Hawaii. The effect of adding bubble injection to the GCM is to increase the argon disequilibrium throughout the thermocline (Figure 4b, dashed line). At the equator, the model predicts approximately 1−2% supersaturation at the sea surface due to surface water warming, with no bubbles at all. This is a good fit to the observations, and so we omit bubble injection from our analysis.

4. Conclusions

[20] Subsurface argon measurements clearly distinguish the diffusive upper thermocline of the equatorial Pacific from the isopycnal subtropics, consistent with thermocline ventilation theory [see *Luyten et al.*, 1983]. However, the lower thermocline, in theory [see *Samelson and Vallis*, 1997] and in the POP model, is ventilated by vertical

Figure 4. ΔAr plotted as a function of water temperature. (a) Blue line and region is pure mixing between 10°C, saturated and 28°C, 1% supersaturated. Red line is the effect of subsurface heating alone, simulated using linear argon saturation dependence in the POP GCM. (b) Solid lines are POP results, using vertical diffusion coefficients of 0.1 (labeled "S"), 0.3, and 1.0 cm^2/s (labeled "F"). Dashed line is 0.3 cm^2/s diffusion with 1% saturation offset imposed at the sea surface due to bubble injection. (c) Solid lines are POP results as in Figure 4b but with ΔAr of 0% disequilibrium imposed for waters colder than 10°C.

diffusion, whereas the lower thermocline in the real ocean appears to ventilate along isopycnals. Additional noble gas disequilibrium data would provide a more definitive test for our understanding of the ventilation of the thermocline.

References

Bieri, R. H. (1971), Dissolved noble gases in marine waters, *Earth Planet. Sci. Lett.*, *10*, 329–333.
Bieri, R. H., and M. Koide (1972), Dissolved noble-gases in east equatorial and southeast Pacific, *J. Geophys. Res.*, *77*, 1667–1676.
Bieri, R. H., M. Koide, and E. D. Goldberg (1966), The noble gas contents of Pacific seawaters, *J. Geophys. Res.*, *71*, 5243–5265.
Bleck, R. (1998), Ocean modeling in isopycnic coordinates, in *Ocean Modeling and Parameterization*, edited by E. Chassignet, and J. Verron, pp. 423–428, Springer, New York.
Craig, H., R. F. Weiss, and W. B. Clarke (1967), Dissolved gases in the equatorial and south Pacific Ocean, *J. Geophys. Res.*, *72*, 6165–6181.
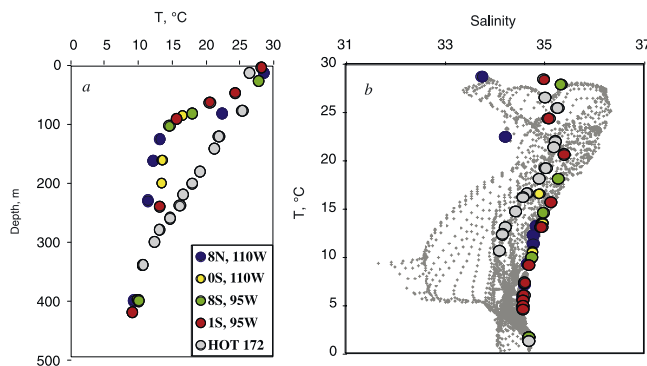
Figure 3. (a) Temperature profiles from the equatorial Pacific and the HOT station. (b) T-S diagram of the Pacific ocean, with data from the equatorial Pacific and HOT superimposed over data from *Levitus et al.* [1993].
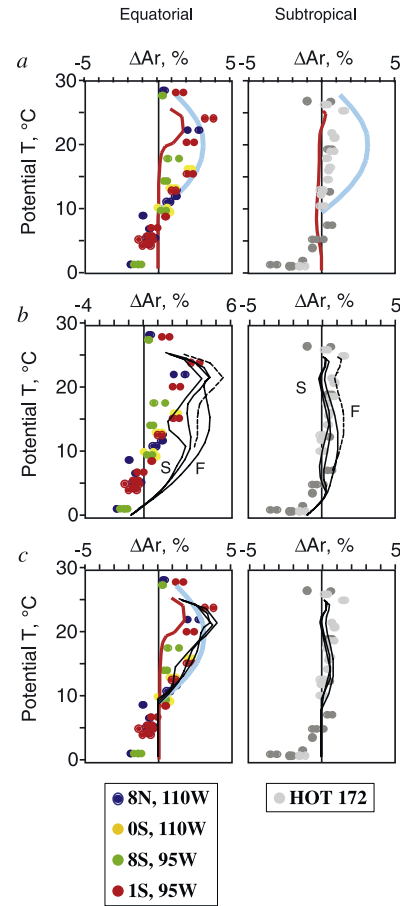
Emerson, S., C. Stump, D. Wilbur, and P. Quay (1999), Accurate measurement of O-2, N-2, and Ar gases in water and the solubility of N-2, *Mar. Chem.*, *64*, 337–347.

Fine, R. A., K. A. Maillet, K. F. Sullivan, and D. Willey (2001), Circulation and ventilation flux of the Pacific Ocean, *J. Geophys. Res.*, *106*, 22,159–22,178.

Gent, P., and J. C. McWilliams (1990), Isopycnal mixing in ocean circulation models, *J. Phys. Oceanogr.*, *20*, 150–155.

Hamme, R. C., and S. R. Emerson (2002), Mechanisms controlling the global oceanic distribution of the inert gases argon, nitrogen and neon, *Geophys. Res. Lett.*, *29*(23), 2120, doi:10.1029/2002GL015273.

Hamme, R. C., and S. R. Emerson (2004), The solubility of neon, nitrogen and argon in distilled water and seawater, *Deep Sea Res., Part I*, *51*, 1517–1528.

Henning, C., D. Archer, and I. Fung (2006), Argon as a tracer of cross-isopycnal mixing in the thermocline, *J. Phys. Oceanogr*, in press.

Ito, T., and C. Deutsch (2006), Understanding the saturation state of argon in the thermocline: The role of air-sea gas exchange and diapycnal mixing, *Global Biogeochem. Cycles*, *20*, GB3019, doi:10.1029/2005GB002655.

Jerlov, N. G. (1976), *Marine Optics*, Elsevier, New York.

Levitus, S., M. E. Conkright, J. L. Reid, R. G. Najjar, and A. Mantyla (1993), Distribution of nitrate, phosphate, and silicate in the world's oceans, *Prog. Oceanogr.*, *31*, 245–273.

Luyten, J. R., J. Pedlosky, and H. Stommel (1983), The ventilated thermocline, *J. Phys. Oceanogr.*, *13*, 292–309.

Murtugudde, R., J. Beauchamp, C. R. McClain, M. Lewis, and A. J. Busalacchi (2002), Effects of penetrative radiation on the upper tropical ocean circulation, *J. Clim.*, *15*, 470–486.

Nurser, A. J. G., R. Marsh, and R. G. Williams (1999), Diagnosing water mass formation from air-sea fluxes and surface mixing, *J. Phys. Oceanogr.*, *29*, 1468–1487.

Samelson, R. M., and G. K. Vallis (1997), Large-scale circulation with small diapycnal diffusion: The two-thermocline limit, *J. Mar. Res.*, *55*, 223–275.

Speer, K. G. (1997), A note on average cross-isopycnal mixing in the North Atlantic ocean, *Deep Sea Res., Part I*, *44*, 1981–1990.

Walin, G. (1982), On the relation between sea-surface heat flow and thermal circulation in the ocean, *Tellus*, *34*, 187–195.

————————————

D. Archer and E. Gehrie, Department of the Geophysical Sciences, University of Chicago, Chicago, IL 60637, USA. (egehrie@mac.com)

S. Emerson and C. Stump, School of Oceanography, University of Washington, Seattle, WA 98195, USA.

C. Henning, Department of Earth and Planetary Sciences, University of California, Berkeley, CA 94720, USA.